Electronic Supplementary Material (ESI) for Journal of Materials Chemistry A.

Electronic Supplementary Information

High-energy Density Nanofiber-based Solid-state Supercapacitors

Daniel Lawrence[a], Chau Tran[a], Arun T. Mallajoysula[b], Stephen K. Doorn[b], Aditya Mohite[b], Gautam Gupta[b,*], and Vibha Kalra[a,*]

[a]Department of Chemical and Biological Engineering, Drexel University, 3141 Chestnut Street, Philadelphia, Pennsylvania 19104, USA

[b]Materials Physics and Applications-11, Los Alamos National Laboratory, NM, 87545

*Corresponding Authors: vk99@drexel.edu (V. Kalra), gautam@lanl.gov (G. Gupta)

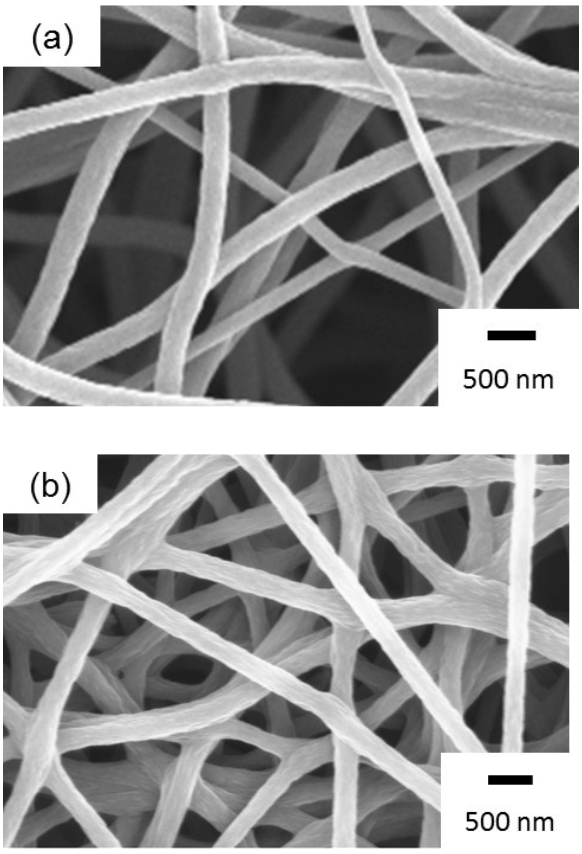

Fig. S1. SEM images of carbon nanofiber mats (a) PCNF and (b) A-PCNF (activated).

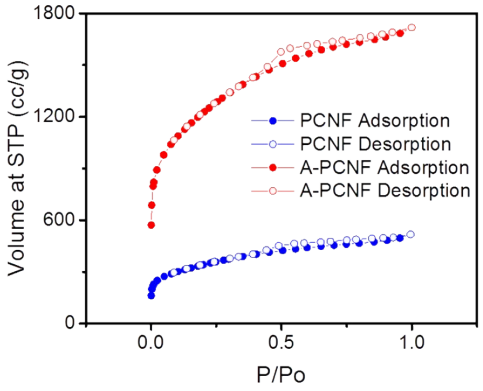

Fig. S2. Adsorption and desorption isotherms for PCNF and A-PCNF.

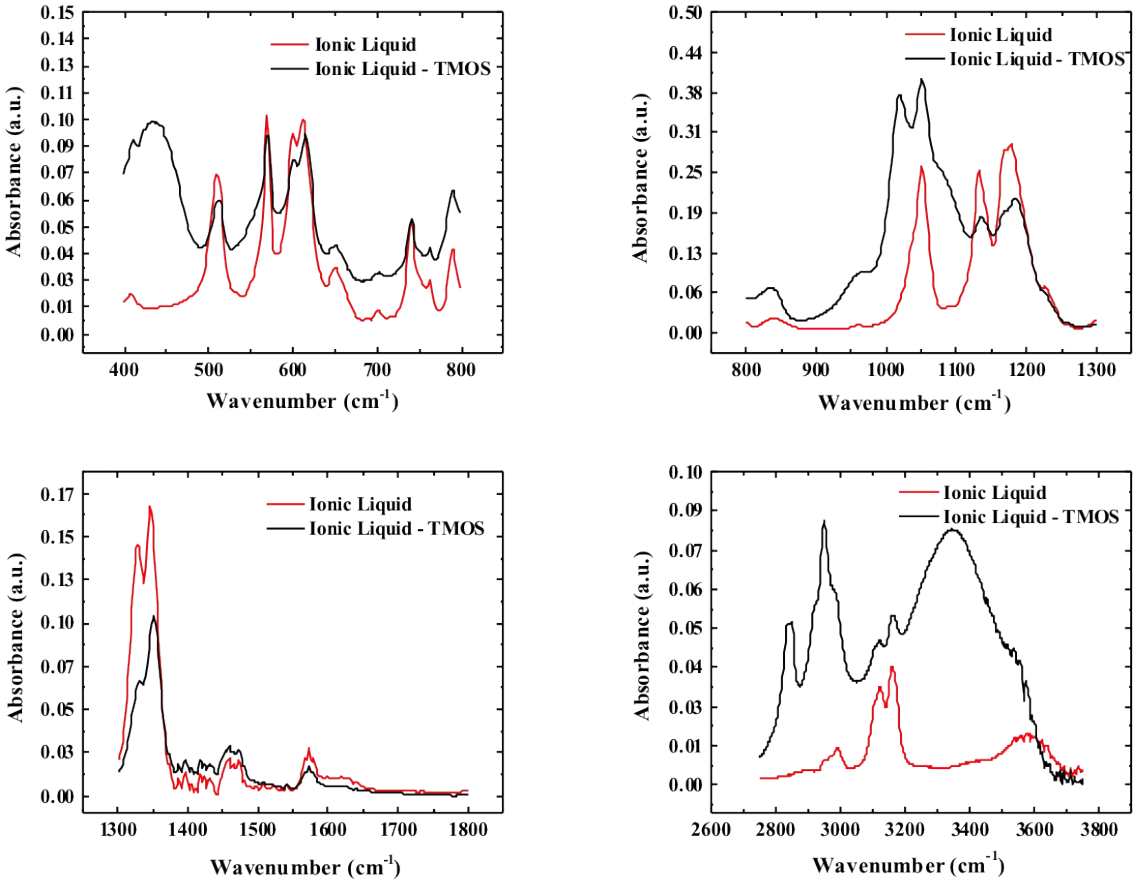

Fig. S3. FTIR spectra of ionic liquid electrolyte with and without TMOS gelation.

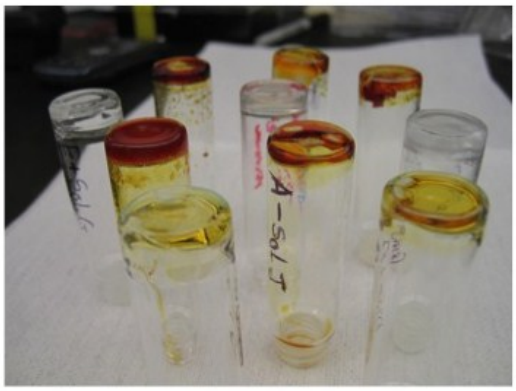

Fig. S4. Pictures of gelled ionic liquid in vials.

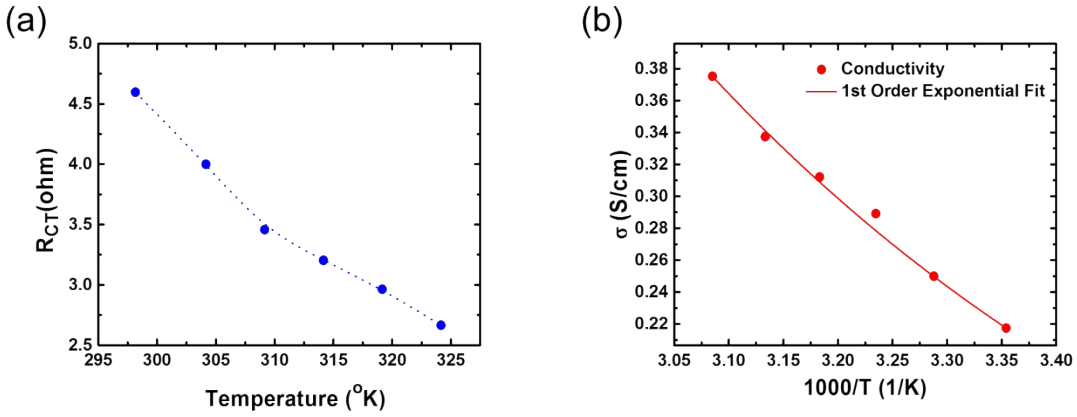

Fig. S5. (a) Variation of charge transfer resistance of solid-state EMIM TFSI electrolyte with temperature. The electrolyte is prepared using tetramethoxysilane (TMOS). (b) Conductivity of EMIM TFSI solid-state electrolyte as a function of inverse temperature. The data fits well to first order exponential, indicating that it tends to follow VFT behavior.

Table S1: Temperature dependence of the charge transfer resistance of solid-state EMIM TFSI electrolyte.

Temperature	Rct (Ω)	1000/T	σ (S/cm)
298.15	4.60	3.35	0.217
304.15	4.00	3.29	0.249
309.15	3.46	3.23	0.289
314.15	3.20	3.18	0.312
319.15	2.96	3.13	0.337
324.15	2.66	3.08	0.375

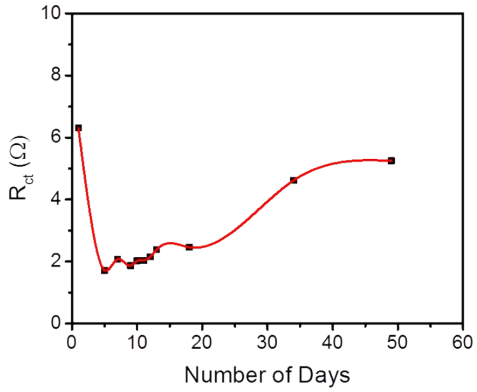

Fig. S6. Time dependence of charge transfer resistance of the solid-state EMIM TFSI electrolyte.

Table S2: Time dependence of the charge transfer resistance of solid-state EMIM TFSI electrolyte.

Day	R_{ct} (Ω)
1	6.305
5	1.715
7	2.079
9	1.8705
10	2.029
11	2.036
12	2.148
13	2.387
18	2.4615
34	4.616
49	5.25

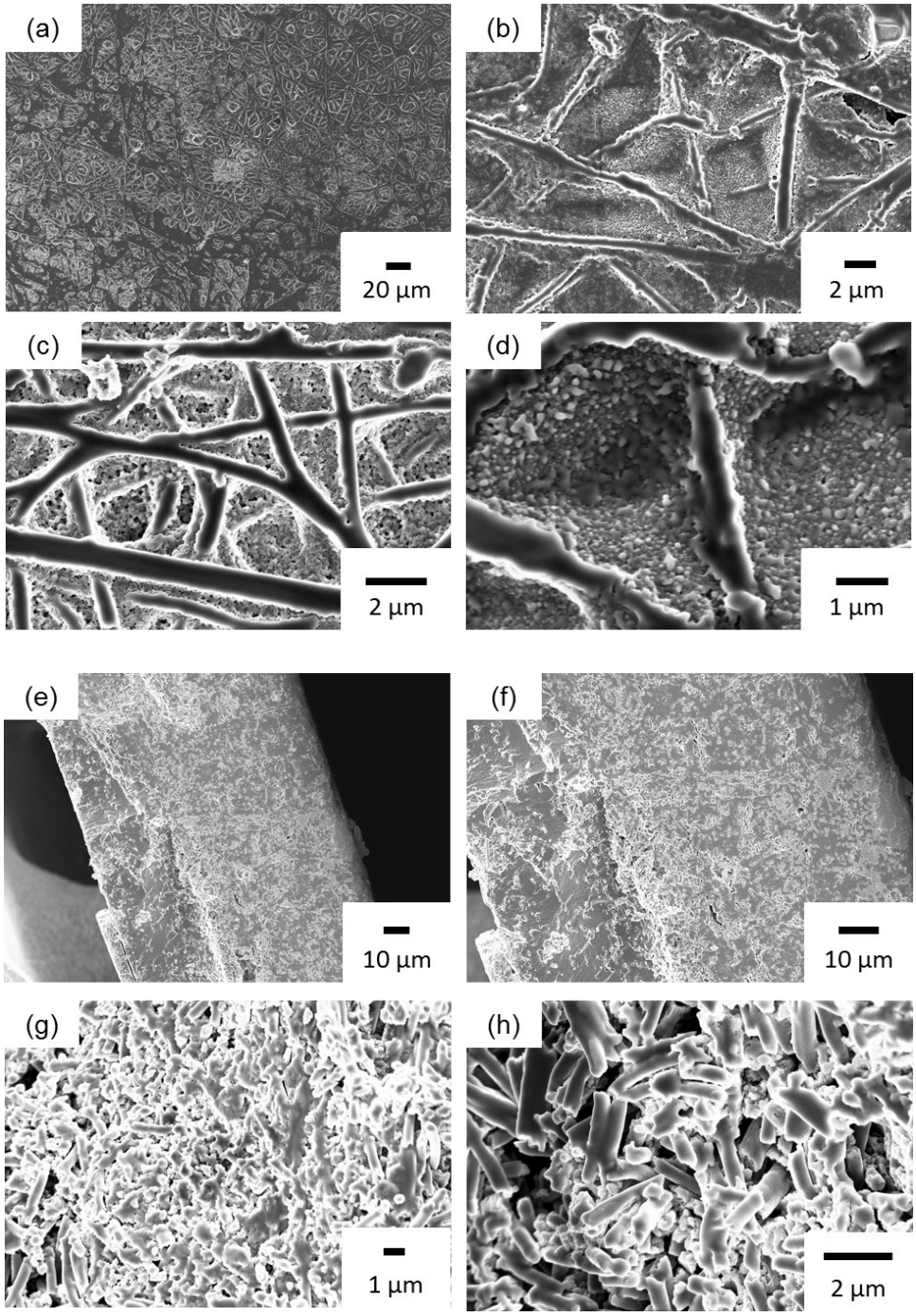

Fig. S7. SEM images of PCNF electrodes filled with solid electrolyte from a (a-d) top-down and (e-h) cross-sectional view.

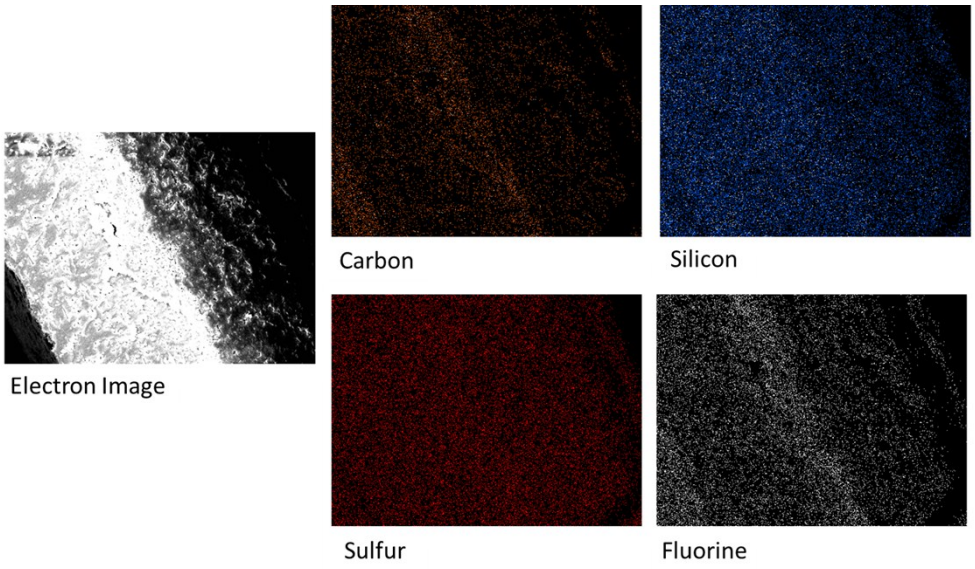

Fig. S8. Solid electrolyte-filled PCNF cross-section EDS showing uniform distribution of TMOS (Si) and EMIM TFSI (S, F).

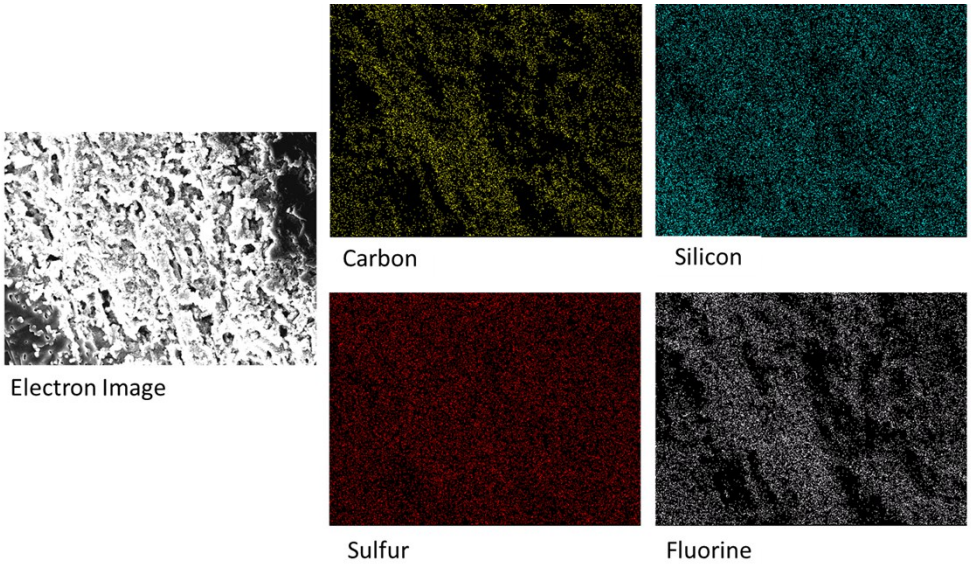

Fig. S9. Solid electrolyte-filled PCNF EDS (top surface) showing uniform distribution of TMOS (Si) and EMIM TFSI (S, F).

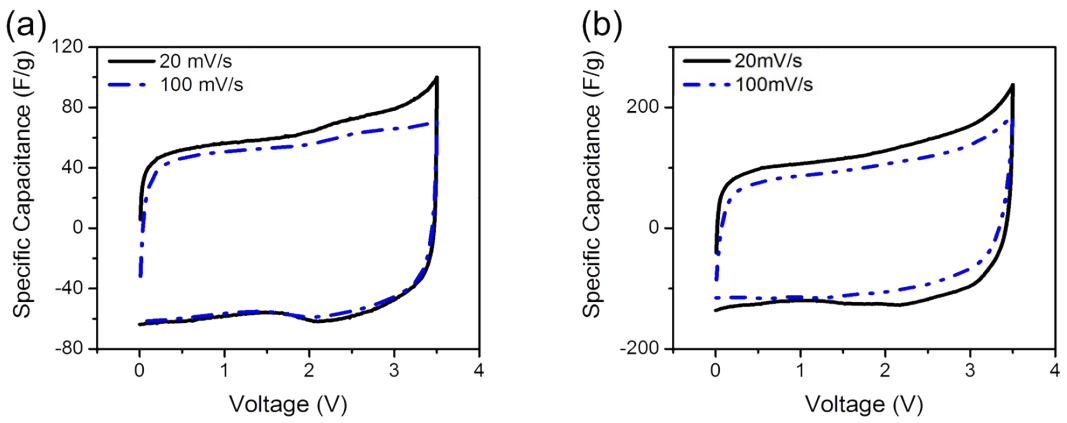

Fig. S10. CV curves of liquid ionic liquid electrolyte devices using the following samples as electrodes (a) PCNF and (b) A-PCNF. PCNF exhibits a capacitance of 59.5 F g^{-1} and 54 F g^{-1} at 20 and 100 mV s^{-1} respectively. A-PCNF exhibits a capacitance of 125 F g^{-1} and 101 F g^{-1} at 20 and 100 mV s^{-1} respectively.

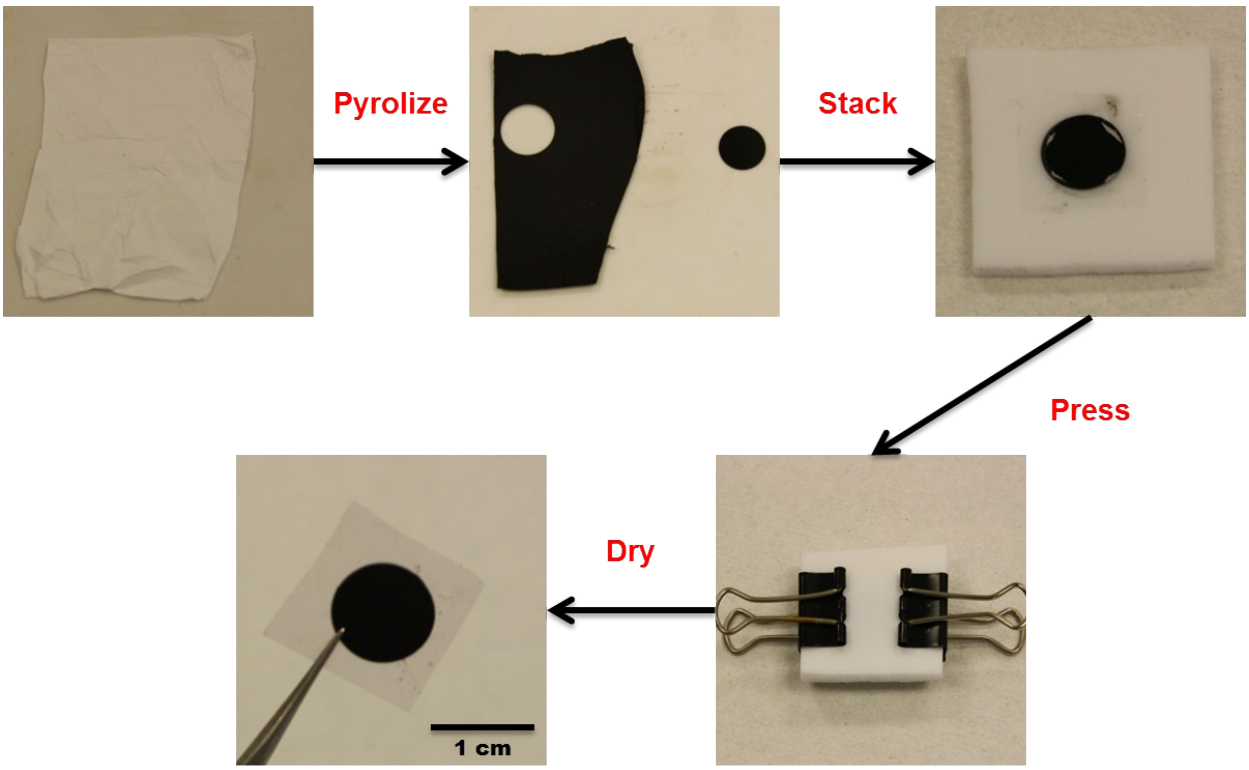

Fig. S11. Schematic showing the detailed step-by-step process used for solid-state device fabrication.

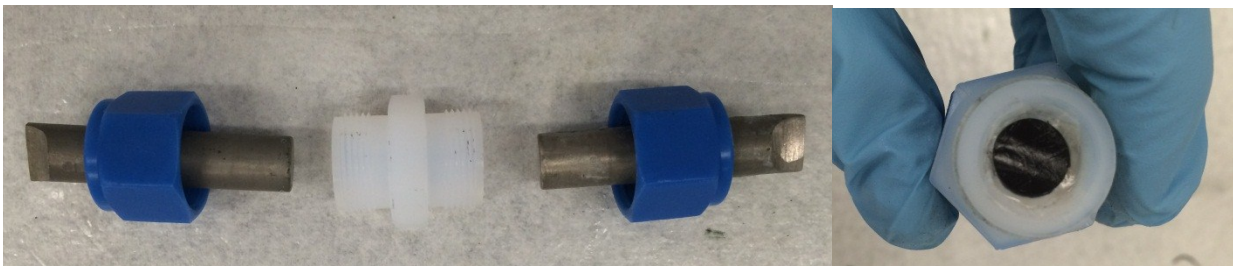

Fig. S12. Photograph representation of the Swagelok cell and the solid-state supercapacitor insert.